Supplement of Atmos. Chem. Phys., 23, 12691–12705, 2023
https://doi.org/10.5194/acp-23-12691-2023-supplement

Atmospheric Chemistry and Physics Open Access

Supplement of

Direct probing of acylperoxy radicals during ozonolysis of α-pinene: constraints on radical chemistry and production of highly oxygenated organic molecules

Han Zang et al.

Correspondence to: Yue Zhao (yuezhao20@sjtu.edu.cn)

S1 Changes in measured RO_2 and closed-shell products as a function of the reacted α-pinene.

The changes of selected RO_2 and the corresponding closed-shell monomers and dimers as a function of the reacted α-pinene are consistent with previous studies (Figure S7) (Zhao et al., 2018). The RO_2 signal increases rapidly when the reacted α-pinene is relatively low, and the increasing rate slows down due to the elevated removal rate of RO_2 via cross-reactions at higher reacted α-pinene (> 20 ppb). The dimers exhibit opposite trends with RO_2. As the reacted α-pinene increases, the increasing rates of the dimers become slightly higher due to the promoted RO_2 cross-reactions. As for the HOM monomers, their signals basically show linear correlations with increasing reacted α-pinene.

S2 Contribution of secondary OH oxidation to the acyl RO_2 formation.

Considering that the secondary OH oxidation of aldehyde products can also contribute to the formation of acyl RO_2 during ozonolysis of α-pinene, kinetic model simulations incorporating secondary OH chemistry were also performed under typical experimental conditions. As shown in Figure S9, the acyl RO_2 $C_9H_{13}O_4$ (C89CO3 in Figure S9a,) and $C_{10}H_{15}O_5$ (C920CO3 in Figure S9b) can be formed from both C-C cleavage/H shift of $C_{10}H_{15}O_4$-RO (Figure 4) and OH oxidation of the first-generation aldehyde products. However, the contributions from secondary OH oxidation are negligible for the two acyl RO_2 species during the whole reaction period. In addition, the acyl RO_2 $C_{10}H_{15}O_4$ (C96CO3) that can be only formed from OH oxidation of pinonaldehyde contributes to only 0.01% and 0.2% of the total $C_{10}H_{15}O_4$-RO_2 and total acyl RO_2 concentration, respectively (not shown). Therefore, the contribution of secondary OH oxidation to acyl RO_2 in this study is minor and the majority of acyl RO_2 species measured here are formed from the ozonolysis channel.

S3 Possible influence of H-scrambling reactions on the behavior of $C_{10}H_{15}O_8$ acyl-RO_2.

It has been suggested that the functionalized acyl RO_2 radicals with an -OOH group could undergo H-scrambling reactions to form peroxy acids at rates of 1×10^3-1×10^5 s^{-1} (Knap and Jørgensen, 2017). Here, we performed a model simulation to evaluate the influence of this reaction on the response of the ring-opened acyl $C_{10}H_{15}O_8$-RO_2 to NO_2 addition. As shown in Figure S14, considering a 1,6 H-shift rate of 1×10^5 s^{-1}, the simulated reduction in total $C_{10}H_{15}O_8$-RO_2 concentration with the addition of 30 ppb NO_2 decreases from 25% to 21% for a $C_{10}H_{15}O_4$-RO_2 yield of 30% (lower limit) and from 31% to 17% for a yield of 89% (higher limit). These results suggest that the H-scrambling reactions of the ring-opened acyl $C_{10}H_{15}O_8$-RO_2 could to certain extent explain the low reduction in its signal upon NO_2 addition.

Table S1 Summary of experimental conditions of α-pinene ozonolysis with the addition of NO_2.

Exp #	α-pinene conc	O_3 conc	NO_2 conc	Reacted α-pinene
1	500	45	0	2.4
2	500	45	3	2.4
3	500	45	7	2.4
4	500	45	10	2.4
5	500	45	15	2.4
6	500	45	20	2.4
7	500	45	30	2.4
8	1000	45	0	4.8
9	1000	45	3	4.8
10	1000	45	7	4.8
11	1000	45	10	4.8
12	1000	45	15	4.8
13	1000	45	20	4.8
14	1000	45	30	4.8
15	2000	45	0	9.3
16	2000	45	3	9.3
17	2000	45	7	9.3
18	2000	45	10	9.3
19	2000	45	15	9.3
20	2000	45	20	9.3
21	2000	45	30	9.3
22	500	180	0	9.6
23	500	180	3	9.6
24	500	180	7	9.6
25	500	180	10	9.6
26	500	180	15	9.6
27	500	180	20	9.6
28	500	180	30	9.6
29	3000	45	0	13.5
30	1000	180	0	18.9
31	2000	180	0	36.8
32*	2000	45	0	5.0

* 500 ppm cyclohexane was added as an OH scavenger in this experiment.

Table S2 Summary of experimental conditions of α-pinene ozonolysis with the addition of NO.

Exp #	α-pinene conc	O_3 conc	NO conc	Reacted α-pinene
33	500	45	3	2.8
34	500	45	7	3.6
35	500	45	10	4.2
36	500	45	15	4.8
37	500	45	20	5.1
38	500	45	30	5.3
39	1000	45	3	5.2
40	1000	45	7	6.0
41	1000	45	10	6.7
42	1000	45	15	7.8
43	1000	45	20	8.6
44	1000	45	30	9.6
45	2000	45	3	9.6
46	2000	45	7	10.4
47	2000	45	10	11.1
48	2000	45	15	12.3
49	2000	45	20	13.4
50	2000	45	30	15.5
51	500	180	3	9.8
52	500	180	7	10.4
53	500	180	10	10.8
54	500	180	15	11.5
55	500	180	20	12.2
56	500	180	30	13.3

Table S3 Major modifications in MCM mechanisms.

#	Reactions	k (s^{-1} or cm^3 $molecule^{-1}$ s^{-1})
1	APINENE + O3 = 0.5 × APINOOA + 0.5 × APINOOB	8.05E-16.*exp(-640./T)
2	APINOOA = Z-APINAOO	KDEC*0.09
3	APINOOA = E-APINAOO	KDEC*0.09
4	APINOOA = C107O2 + OH	KDEC*0.45
5	APINOOA = C109O2 + OH	KDEC*0.37
6	APINOOB = Z-APINBOO	KDEC*0.10
7	APINOOB = E-APINBOO	KDEC*0.10
8	APINOOB = PINONIC	KDEC*0.16
9	APINOOB = C10H15O4KBRO2 + OH	KDEC*0.49
10	APINOOB = C10H15O4RBRO2 + OH	KDEC*0.5*0.3
11	C107O2 = C10H15O6R1RO2	0.14
12	C109O2 = C10H15O6R1RO2	0.02
13	C10H15O4KBRO2 = C10H15O6KBRO2	0.29
14	C10H15O4RBRO2 = C10H15O6RBRO2	1
15	RO2 + NO2 = ROONO2	7.5E-12
16	ROONO2 = RO2 + NO2	5

Table S4 Wall loss fractions of OH, HO_2, and RO_2 radicals, as well as HOM monomers and dimers under different reaction conditions

Species	D_{gas} (cm^2 s^{-1})	k_{wall} (s^{-1})	Wall loss fractions (%)			
			500 ppb αp +45 ppb O_3	1 ppm αp+45 ppb O_3	2 ppm αp+45 ppb O_3	500 ppb αp+180 ppb O_3
OH	0.23	0.0537	0.14	0.11	0.08	0.08
HO_2	0.15	0.0354	9.08	6.71	4.89	4.74
C_7-RO_2	0.07	0.0171	13.9	11.9	9.8	9.6
C_8-RO_2	0.07	0.0171	25.5	21.5	18.0	17.7
C_9-RO_2	0.07	0.0171	16.4	16.2	14.5	14.3
C_{10}-RO_2	0.05	0.0125	11.5	9.3	7.4	7.3
C_7-HOM	0.07	0.0171	24.3	23.3	22.5	22.3
C_8-HOM	0.07	0.0171	34.7	31.0	28.1	27.8
C_9-HOM	0.07	0.0171	29.0	27.5	26.1	25.9
C_{10}-HOM	0.05	0.0125	22.3	20.3	18.6	18.4
$C_{14\text{-}15}$-dimers	0.05	0.0125	33.1	30.5	27.8	27.6
$C_{16\text{-}19}$-dimers	0.03	0.0079	25.4	22.6	20.0	19.7
C_{20}-dimers	0.03	0.0079	17.5	15.8	14.4	14.2

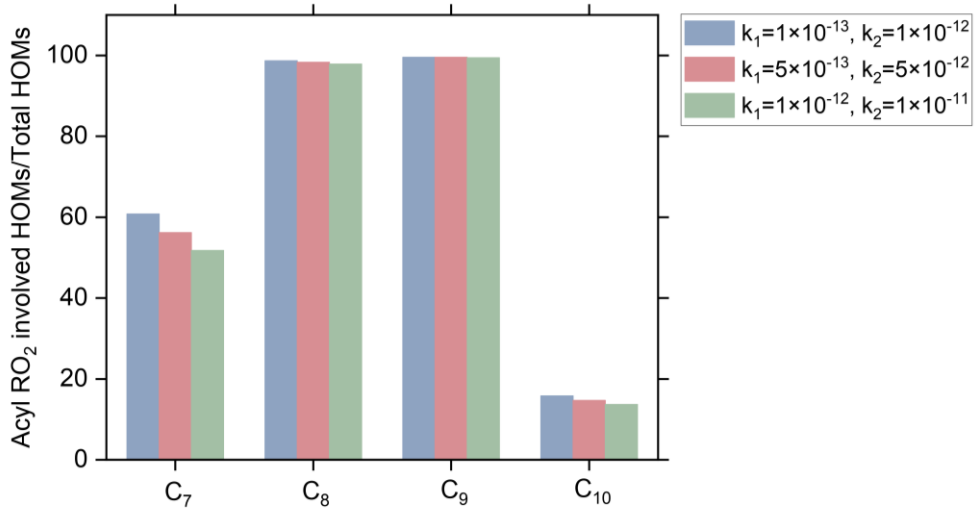

Figure S1 Influences of the dimer formation rate on the acyl RO_2-involved HOM formation. k_1 and k_2 are the dimer formation rates for alkyl and acyl RO_2, respectively, and the unit is cm^3 $molecule^{-1}$ s^{-1}.

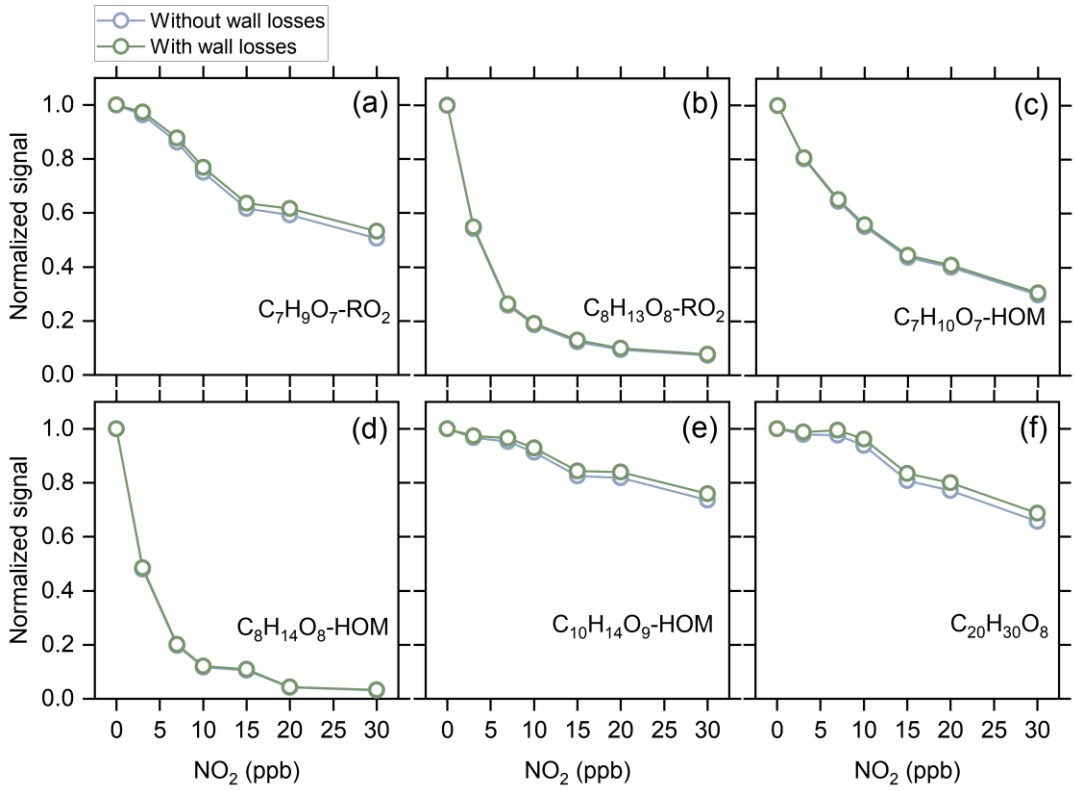

Figure S2 Normalized signal of typical RO_2, HOM monomers and dimers as a function of the added NO_2 concentration with/without considering wall losses (Taking Exps 8-14 as an example).

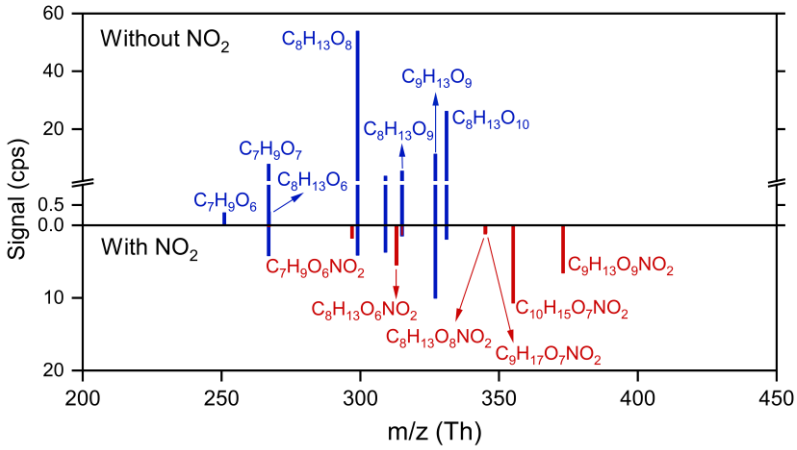

Figure S3 Signals of measured acyl RO_2 and the related $RC(O)OONO_2$ with and without the addition of NO_2 (Exps 8 and 14).

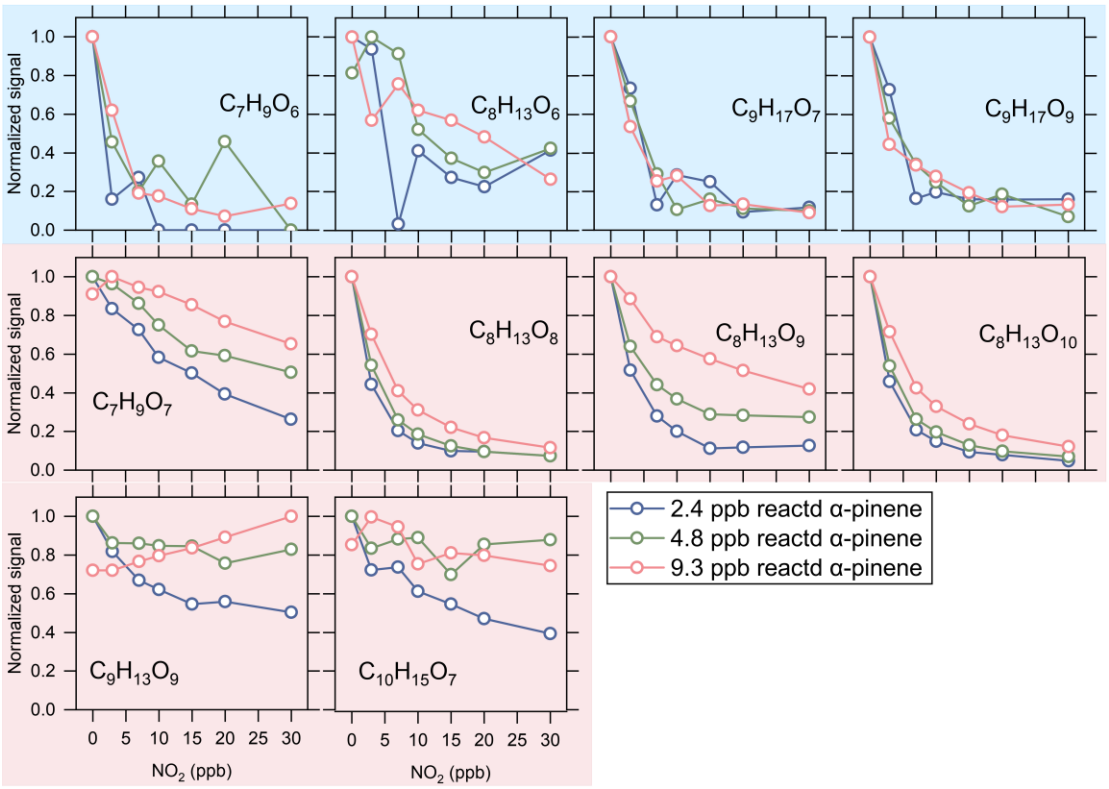

Figure S4 Normalized signal of the measured acyl RO_2 as a function of the added NO_2 concentration (Exps 1-21). The data are categorized according to the effects of reacted α-pinene on the decreasing extents of acyl RO_2 signal, which are indicated by different background colors (blue: no obvious effects, pink: the decreasing extent becomes lower when reacted α-pinene increases).

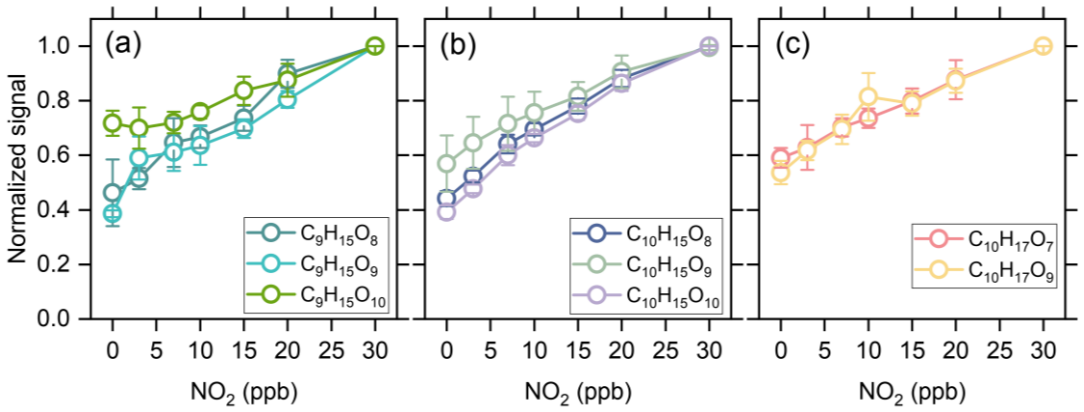

Figure S5 Averaged normalized signal of the measured alkyl RO_2 as a function of the added NO_2 concentration (Exps 1-28).

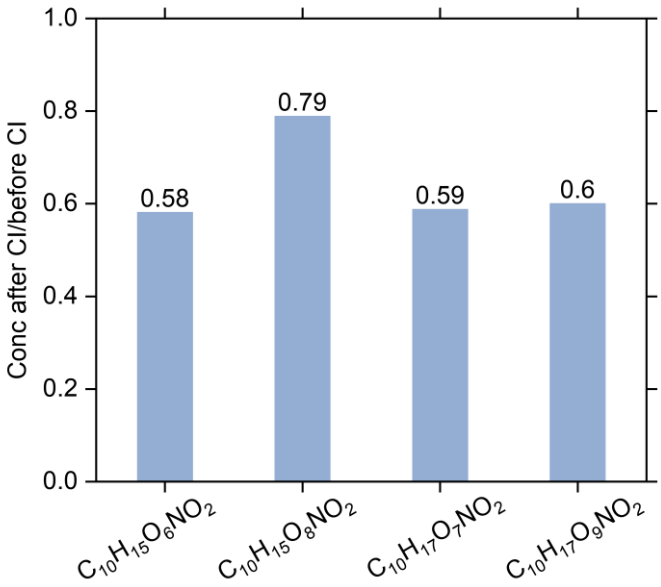

Figure S6 Ratio of simulated concentration of $ROONO_2$ after leaving the chemical ionization inlet to the concentration before into the chemical ionization inlet (abbreviated as CI in the figure, the experimental conditions are same as Exp 14), the acyl RO_2 $C_{10}H_{15}O_8$ reported by Iyer et al. (2021) is included in the model, therefore the decomposition of the whole $ROONO_2$ is relatively lower.

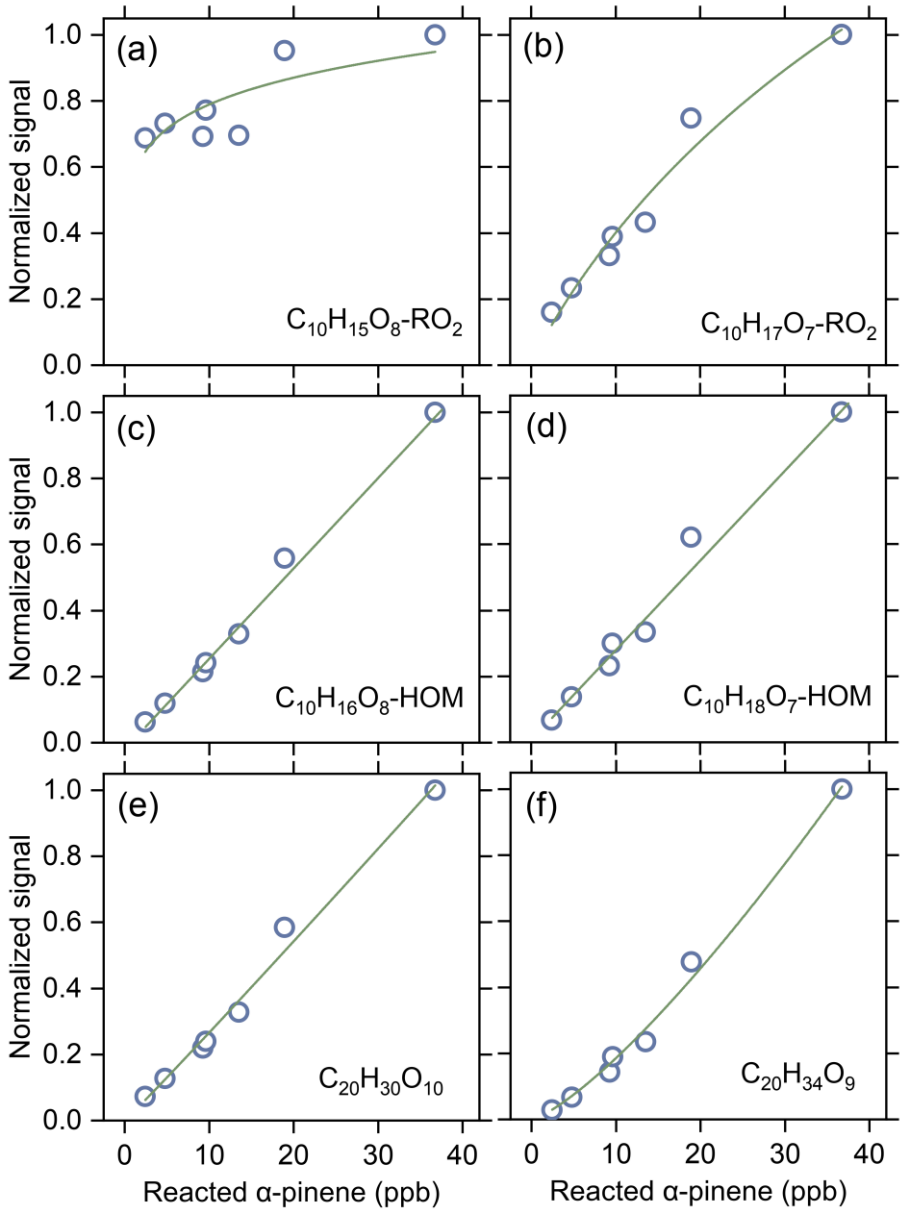

Figure S7 Normalized signal of selected RO_2 as well as closed-shell monomers and dimers as a function of the reacted α-pinene (Exps 1, 8, 15, 22, and 29-31).

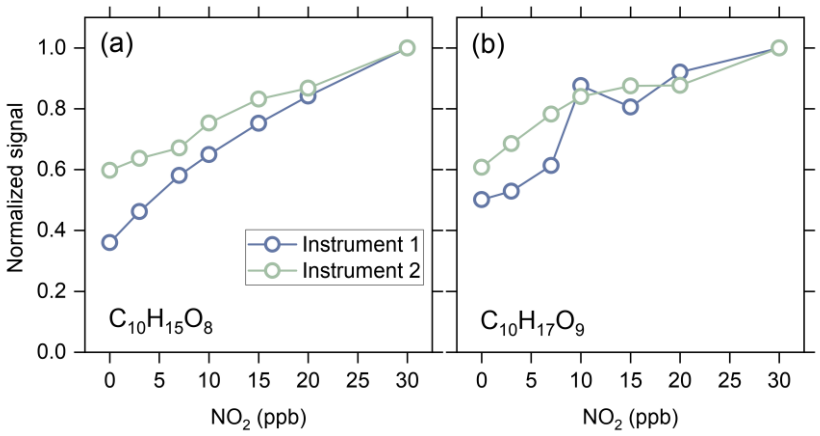

Figure S8 Changes of typical alkyl RO_2 signal with different NO_2 concentration measured by two nitrate-CIMS under the same experimental conditions (Exps15-21). Instrument 1 is the nitrate-CIMS we used in this study.

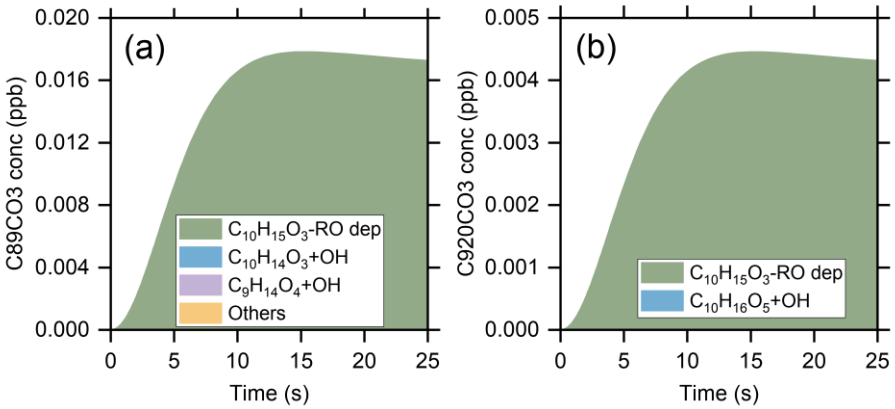

Figure S9 Simulated contribution of different processes to the formation of (a) $C_9H_{13}O_4$ (C89CO3) and (b) $C_{10}H_{15}O_5$ (C920CO3) acyl-RO_2 during ozonolysis of α-pinene (Exp 22, 500 ppb α-pinene + 180 ppb O_3).

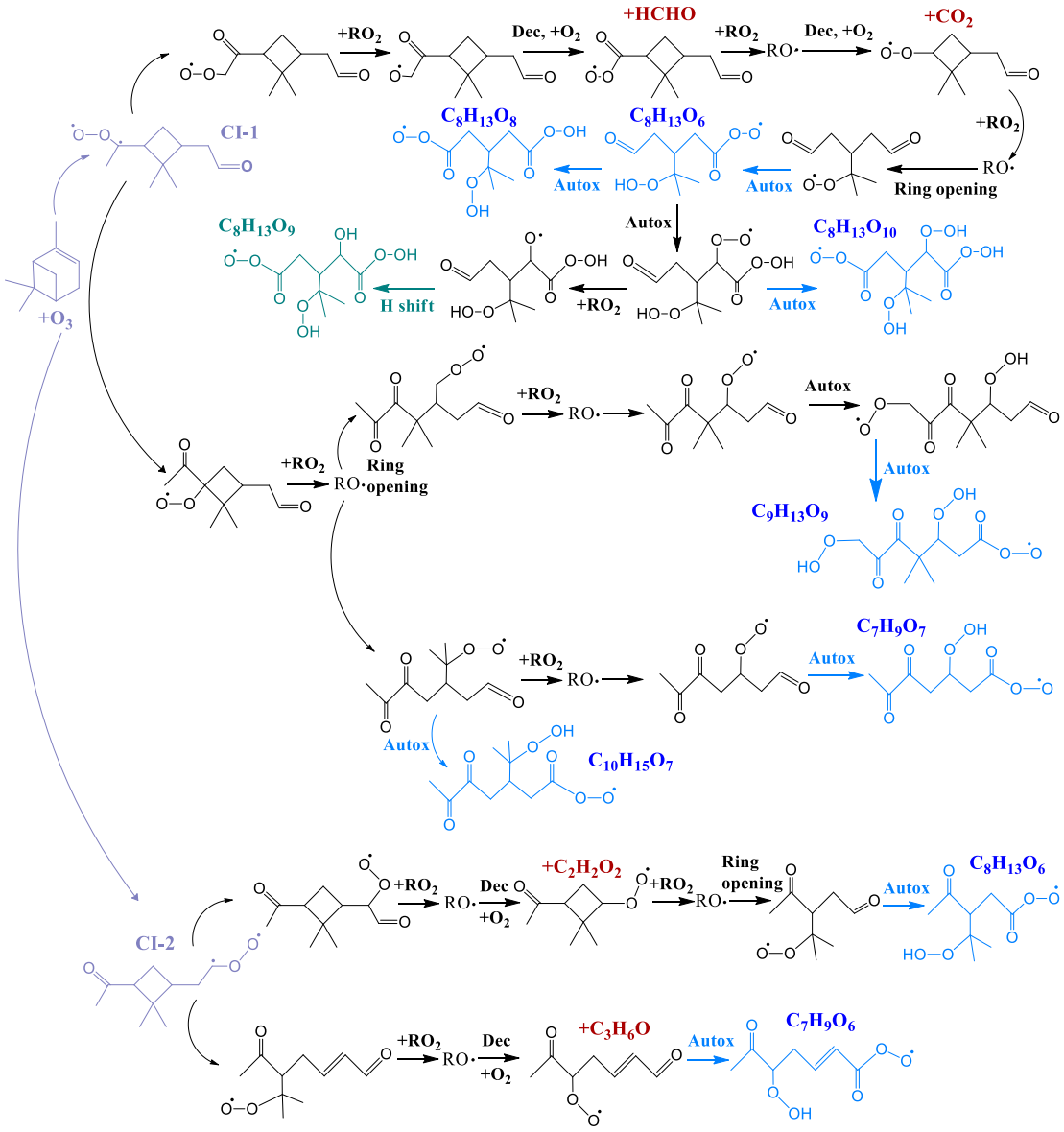

Figure S10 Formation mechanisms of the acyl RO_2 measured in this study.

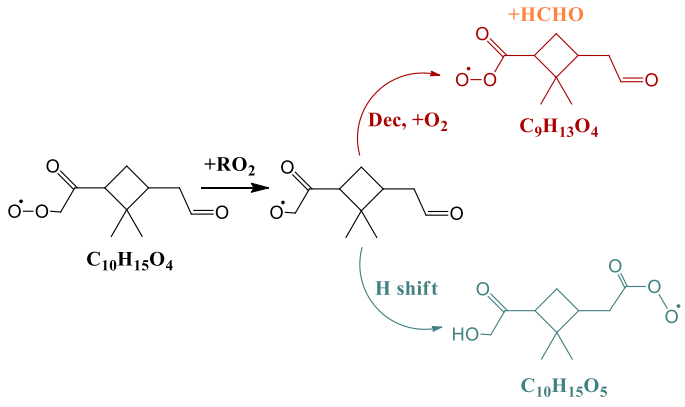

Figure S11 Formation pathways of the acyl RO_2 with oxygen atoms less than 6 in default MCM v3.3.1.

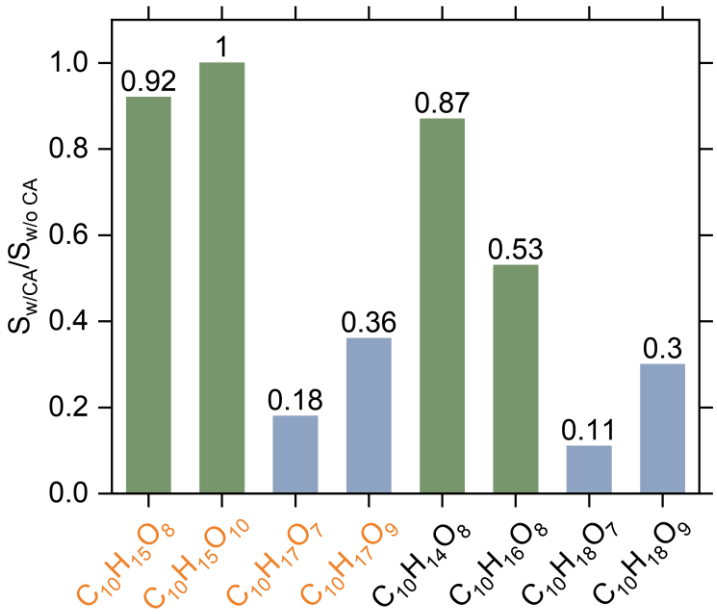

Figure S12 Relative changes in signal of typical C_{10} RO_2 and HOM monomers due to the addition of 500 ppm cyclohexane (Exp 32), the yellow species are RO_2 radicals.

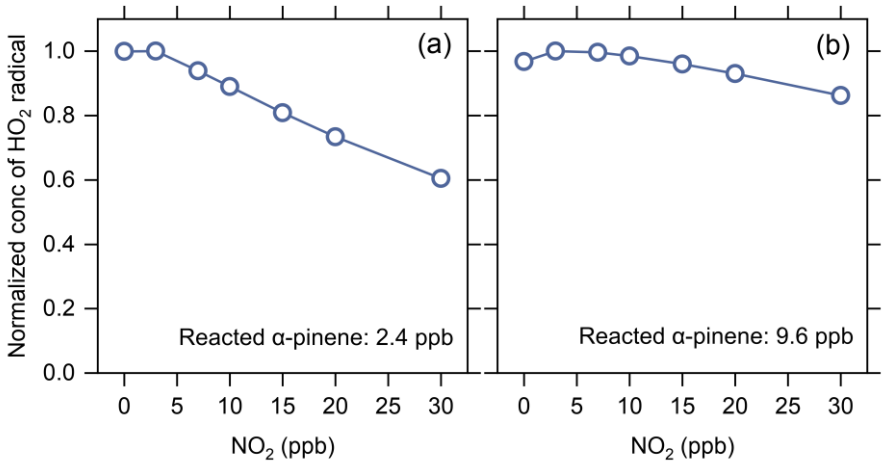

Figure S13 Normalized simulated concentration of the HO_2 radicals as a function of NO_2 concentration under low (2.4 ppb, a) and high (9.6 ppb, b) reacted α-pinene conditions.

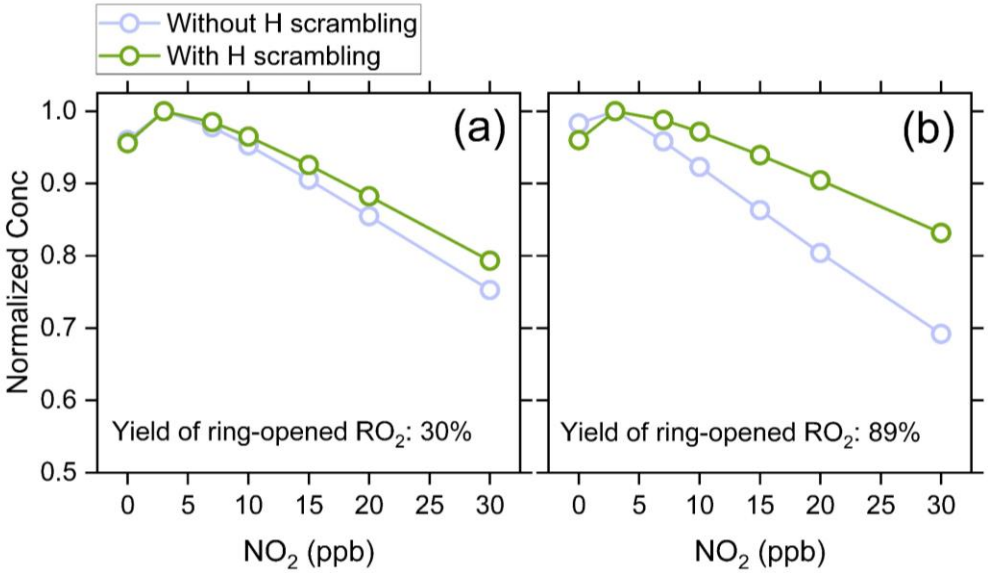

Figure S14 Simulated influences of the H-scrambling reaction on the behavior of the ring-opened acyl $C_{10}H_{15}O_8$-RO_2 as a function of added NO_2 concentration (Exps 8-14). A 1,6 H-scrambling rate of 1×10^5 s^{-1} and an alkyl RO_2+NO_2 rate coefficient of 5×10^{-12} cm^3 $molecule^{-1}$ s^{-1} were used in the model.

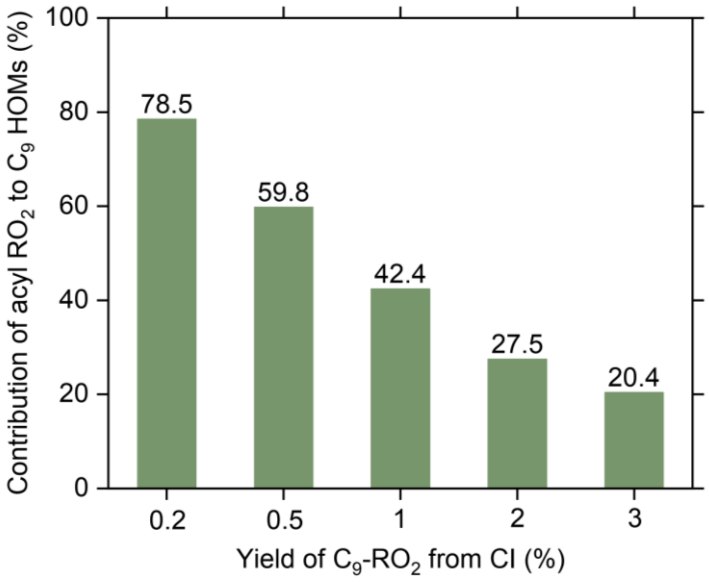

Figure S15 Influences of $C_9H_{15}O_3$-RO_2 production from one of the CIs on the formation of C_9 acyl RO_2 related HOMs (Taking Exp 8 as an example).

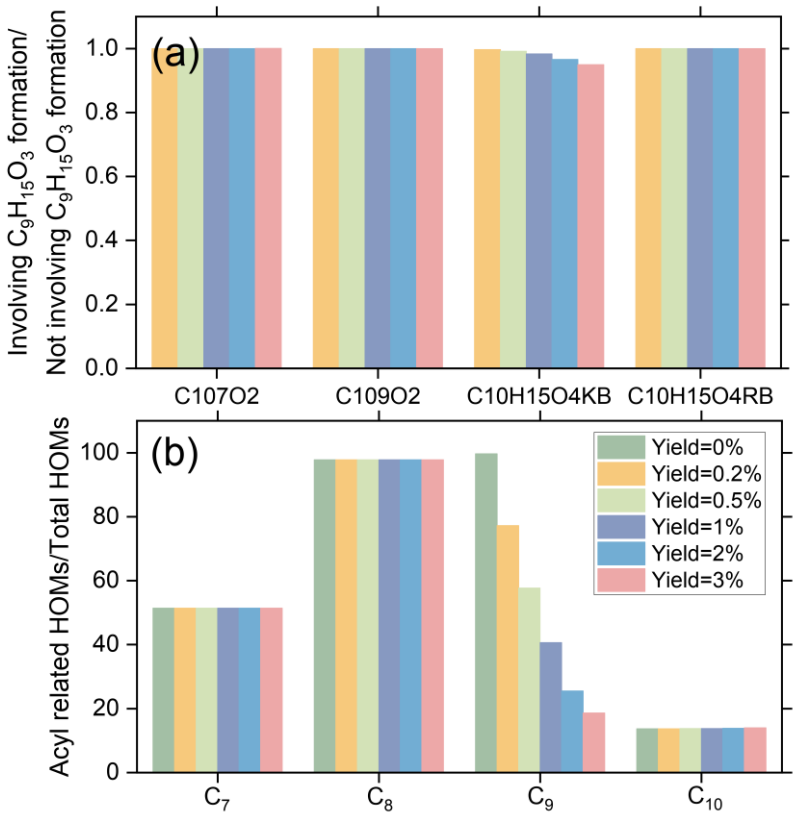

Figure S16 Influences of $C_9H_{15}O_3$-RO_2 production on (a) the yield of $C_{10}H_{15}O_4$-RO_2 and (b) the contribution of acyl RO_2 to total C_7-C_{10} HOMs (Taking Exp 8 as an example). The C10H15O4KB and C10H15O4RB denote a ring-retaining and a ring-opened $C_{10}H_{15}O_4$-RO_2, respectively (see Table S3 and the main text).

References

Iyer, S., Rissanen, M. P., Valiev, R., Barua, S., Krechmer, J. E., Thornton, J., Ehn, M., and Kurten, T.: Molecular mechanism for rapid autoxidation in alpha-pinene ozonolysis, Nat. Commun., 12, 878, https://doi.org/10.1038/s41467-021-21172-w, 2021.

Knap, H. C. and Jørgensen, S.: Rapid Hydrogen Shift Reactions in Acyl Peroxy Radicals, J. Phys. Chem. A, 121, 1470-1479, 10.1021/acs.jpca.6b12787, 2017.

Zhao, Y., Thornton, J. A., and Pye, H. O. T.: Quantitative constraints on autoxidation and dimer formation from direct probing of monoterpene-derived peroxy radical chemistry, Proc. Natl. Acad. Sci. U. S. A. , 115, 12142-12147, https://doi.org/10.1073/pnas.1812147115, 2018.